UNIVERSITÄT FÜR BODENKULTUR WIEN
University of Natural Resources
and Life Sciences, Vienna

Protectiveness of a trivalent, recombinant, adjuvanted neuraminidase-based influenza vaccine against virus challenges in the mouse model

submitted by

Lukas PUCHER, BSc

Research Paper for the Austrian Marshall Plan Scholarship

Medellín, December 2022

Supervisors:
Univ.Prof. Dipl.-Ing. Dr.rer.nat. Reingard Grabherr
Department of Biotechnology
University of Natural resources and Life Sciences, Vienna

Prof. Dipl.-Ing. Dr.rer.nat. Florian Krammer
Department of Microbiology
Icahn School of Medicine at Mount Sinai

Affidavit

I hereby declare that I have authored this work independently and have not used any assistance other than permitted. The work contained herein is my own except where explicitly stated otherwise. All ideas taken in wording or in basic content from unpublished sources or published literature are duly identified and cited, and the precise references included.

I further declare that this work has not been submitted, in whole or in part, in the same or a similar form, to any other educational institution as part of the requirements for an academic degree.

I hereby confirm that I am familiar with the standards of Scientific Integrity and the guidelines of Good Scientific Practice and that this work fully complies with these standards and guidelines.

Medellín, 13/12/2022 Lukas PUCHER *(manu propria)*

“Mei Bier is ned deppat!”
Mundl, Vienna, 1978

Preface

This work was funded by the Austrian Marshall Plan Foundation fellowship.

Acknowledgments

I want to thank, first and foremost, Jordan and Irene for supporting me on so many scientific levels. Of course, I want to show my gratitude to Madhu and Ben, who produced the NA constructs. To Zeli, who lets me participate in this project. Kirsten, for providing the adjuvant and conjugating the proteins. Edu, for providing the Switzerland H3N2 strain. Florian, who allowed me to be here and showed me how to fish in the Atlantic Ocean. Reingard, agreed to supervise me.

Table of content

Abstract

Since approximately 500 years, humans have suffered from pandemic influenza. And to this day, influenza is still a significant danger to human health. In particular, children without previous exposure and the elderly with immunosenescence are threatened. The current influenza vaccine induces a humoral immune response focused on the immunodominant head domain of the hemagglutinin (HA). Since the head of HA is highly variable, this immunity is narrow and strain-specific. Vaccine mismatch with the circulating strains and egg adaptation of the vaccine strains can lower the vaccine effectiveness drastically. The neuraminidase (NA), the second major surface glycoprotein of influenza, mutates slower than the HA. Humoral immunity against NA has been shown to be an independent correlate of protection, and antibodies targeting the NA have been found to reduce viral shedding and to stop transmission. Current influenza vaccines contain variable and not standardized amounts of NA. Only a small proportion of antibodies elicited by the current seasonal influenza vaccines targets the NA. The aim of this work is the testing of a stand-alone recombinant, adjuvanted NA-based influenza vaccine. For this purpose, the three NAs of the current, among humans circulating influenza strains, were chosen, stabilized with a tetramerization domain of the measles phosphoprotein, and expressed in insect cells. Since recombinant proteins alone show low immunogenicity, the NAs were conjugated to alum using a linker containing polyethyleneglycol and phosphoserine. This formulation was further adjuvanted with saponin/MPLA nanoparticles (SMNPs). As a comparison, the well-known oil-in-water emulsion adjuvant AddaVax was used. To test these different vaccine formulations, mice were vaccinated in a prime-boost regime and challenged with seasonal influenza strains (pH1N1, H3N2, and B-Victoria). As a heterologous challenge, the probably extinct B-Yamagata lineage and H5N1 were used. This work shows that the SMNP/alum formulation could not break antigenic competition between NAs in a trivalent formulation. However, the vaccine protected against all homologous and partly heterologous challenges. The author suggests using a higher antigen dose and/or a different adjuvant for further investigations.

1. Introduction

1.1. Influenza

Influenza virus is a segmented, negative-stranded RNA virus that belongs to the family of *Orthomyxoviridae*[1]. The segmented genome of the genera influenza A and B consists of 8 parts that encode at least 11 proteins. Two of these proteins are the surface glycoproteins hemagglutinin (HA) and neuraminidase (NA). By now, 18 HAs and 11 NAs of influenza A have been classified according to serological cross-reactivity[2]. Influenza B glycoproteins are not classified in subtypes but in Victoria and Yamagata like.

The role of the trimer HA is receptor binding and membrane fusion. The HAs of human influenza viruses bind preferably to the sialic acid N-acetylneuraminic acid. HA is translated as an HA0 precursor that needs to be cleaved in HA1 and HA2 to become functional. The cleavability of HAs defines in part its host cell range and, therefore, to some degree, disease severity (HAs with a polybasic cleavage side can be functionalized in many cell types and therefore cause systemic disease)[3,4]. Remarkable about the HA is its sequence variability (that can be lower than 50%) while keeping the same structure. The fusion process of the HA requires low pH. Therefore, membrane fusion can only take place in endosomes. The possible mechanisms for internalization are via macropinocytosis, through clathrin-coated pits, through caveolae, or via nonclathrin and noncaveolae pathways[3,5]. After a pH drop in the endosome, the HA undergoes a structural change by exposing its HA2 N-terminal fusion peptide. The fusion peptides of several HAs penetrate together the endosomal membrane and form a pore. The M2 ion channel in the envelope allows H^+ ion influx that facilitates uncoating and helps with the release of viral ribonucleoprotein (RNP) complexes into the cytosol[5,6].

Viral ribonucleoprotein (vRNP) complexes consist of viral RNA (vRNA) and nucleocapsid protein (NP), but also PB1, ,PB2 and PA that bind to the complementary ends at the vRNA segments and form the characteristic panhandle structure[7]. Predominantly NP, but also on the other proteins in the ,vRNP carry signal patterns on their surface that causes the import of the whole vRNP into the nucleus. In the nucleus, PB1, PB2, and PA form together the RNA-dependent RNA polymerase (RDRP). Transcription starts with cap-snatching from host pre-mRNA transcripts facilitated by the binding activity of PB2 and the endonuclease activity of PA. Elongation of mRNA and later copy RNA (cRNA) and vRNA is catalyzed by the PB1 subunit. The poly(A) tail is produced by stuttering of the RDRP caused by steric hindrance. It is not entirely understood how the RDRP changes from mRNA to vRNA production. Sufficient levels of RNP-forming proteins seem to be required[8].

The different affinities of HA towards either Siaα2,6Gal or Siaα2,3Gal determines the host range of influenza partly. A typical infection starts by binding of HA to a sialic acid sugar molecule on top of a galactose on the cell surface. The bond between sialic acid and galactose differs between species and body parts. While in humans, Siaα2,6Gal is prevalent in the upper respiratory tract, Siaα2,3Gal oligosaccharides can be found on nonciliated cells in the lower respiratory tract. In pigs, epithelial cells in the trachea contain both Siaα2,3Gal and Siaα2,6Gal. Birds, the primary reservoir of the influenza virus, where influenza replicates in the intestine, have predominantly Siaα2,3Gal but also Siaα2,6Gal oligosaccharides. It is thought that pigs or birds with cells of Siaα2,6Gal and Siaα2,3Gal glycosylated cells in proximity allow adaptation of HA with preferred Siaα2,3Gal binding to higher affinity towards Siaα2,6Gal oligosaccharides[9]. This oligosaccharide distribution can partly explain the severe pneumonia observed after infection with some avian influenza viruses and the limited human-to-human transmission of humans infected with H5N1 (avian). The model of sialic acid as the primary determinant of virus entry can partly explain the host range. Despite that, the oligosaccharide sequence and structure below the Siaα2,3Gal/Siaα2,6Gal may also influence the interaction with HA[10].

1.2. Influenza vaccines

Seasonal Influenza is responsible for 291 243-645 832 deaths annually, with the highest mortality rates in sub-Saharan Africa, Southeast Asia, and among people above the age of 75. After infection, the long-lived human humoral immune response is mainly directed against HA and NA[11]. To evade this response, subsequent strains must undergo antigenic evasion. Antigenic drift describes the occurrence of mutations on crucial epitopes on the HA or NA. The adoption of entirely novel antigens to the human population through re-assortment with an animal strain is termed antigenic shift[1].

Currently, available vaccines are standardized for their HA content[12]. In the US, several quadrivalent (consisting of an H1N1pdm09, H3N2, B-ViB-Yamagata-likemagata like HA) influenza vaccines are available. Except for FluMist, all vaccines are administered over the intramuscular route. The traditional influenza vaccine is based on virions grown in eggs. The HA and NA encoding genome segments of the viruses expected to circulate are reassorted with the internal segments of A/Puerto Rico/8/1934 (PR8), a virus that grows to high titers in eggs. After harvest and clearing of the allantoic fluid via low speed centrifugation, virions are concentrated via ultracentrifugation. To reduce reactogenicity, detergents are used to split the virion. Several vaccines are available based on this technology: Fluzone, consisting of 15 µg of each respective HA, is licensed for six months and older. Fluzone is approved for the age >65 years and consists of 4 times the HA dose of conventional influenza vaccines (60 µg)[13]. Fluad, is va accine containing 15 µg per HA per dose and adjuvanted with MF59. MF59 is an oil-in-water emulsion adjuvant. Added to the vaccin,e it can decrease hospitalizations compared to the standard dose vaccine. It has been shown that MF59 can increase breath and titer of the antibody response[14]. FluMist is also an egg-grown vaccine but administered as a nasal spray. The vaccine virus is cold-adapted (25 °C) which restricts replication to the upper respiratory tract. Despite the induction of an IgA response and broader relative breath[15], efficacy against disease appears to be lower than the inactivated influenza vaccine (IIV) in children against $H1N1_{pdm09}$ but not against H3N2 or influenza B[16,17]. Flucelvax is an IIV containing virus grown in Madin-Darby Canine Kidney (MDCK) cells. This different production process is meant to circumvent the problem of virus adaptions to eggs. Flublok is the only shot not based on grown up influenza virus but on recombinantly produced HA (rHA). 45 µg HA are used per dose[18].

Estimations of mortality in children are broad and range from 9243 to 105 690 deaths worldwide annually[19]. Vaccine effectiveness (VE) against death in children is estimated to range from only 65%[20] to 75%. Overall, VE in the US was estimated to range from 10% to 60% between 2004 and 2022[21] but was particularly low in the previous years: 14%-39% from 2017-2022. Besides the low VE, several other issues remain with the annual influenza vaccine. Currently, available influenza vaccines induce a narrow, on variable parts of the head of HA focused, short-lived immune response[11]. Since most individuals have encountered influenza in their life (it is estimated that adults get infected every 5-10 years), most individuals have pre-existing immunity. It has been found that IIVs activate memory B-cells that evolve into antibody-secreting cells that produce antibodies against variable domains of the HA head domain[22]. This makes the immune response strain-specific. Another problem is the possible mismatch between the circulating strain and the vaccine. When the WHO chooses the vaccine strains in February, the actual circulating strains in the northern hemisphere are unknown. A mismatch between the vaccine and circulating strain can significantly decrease the VE. The narrowness of the immune response towards variable domains is probably caused by antigenic seniority – a result of the unique history of influenza infections and administered vaccines. Pre-existing circulating antibodies shield epitopes from recognition of B-cells - especially on conserved parts of administered antigen[23].
The need for annual influenza vaccines is not only a problem in the wealthy part of the planet. Vaccinating disadvantaged parts of the world with vaccines that require only one shot, like the Measles-Mumps-Rubella (MMR) vaccine remains a problem. An annual vaccine in some parts

of the world is illusory in the current political and economic situation. Apart from these logistic reasons, annual vaccination could reduce vaccine effectiveness in general[24]. Possibly, through the mechanism of antigenic seniority as described previously. This public health problem shows the need for better influenza vaccines.

1.3. Neuraminidase-based vaccines

Neuraminidase is a tetrameric type II transmembrane glycoprotein on the surface of influenza A and B virions. It is an enzyme showing sialidase activity. Thus, it cleaves sialic acid from glycans. That function has been termed receptor-destroying activity[3,12]. NA is needed at several stages of the viral life cycle. Therefore, NA-inhibiting (NI) antibodies have multiple opportunities to interfere. By cleavage of sialic acid from mucins, NA keeps the virion from being trapped before reaching the surface of epithelial cells. After reaching a target cell, the virion can be trapped on non-receptor glycans of the glycocalyx. Arguably NA has one of its most essential rolls at the virion budding when it cleaves attached HAs off the host cell. Inhibiting these mechanisms can stop infection and transmission: *In vitro* experiments have shown a 20 to the 500-fold reduction of infection of human upper airway epithelium cells after inhibiting NA[25]. Oral vaccination of guinea pigs prevented transmission of influenza B[26]. Antibodies binding the active site of the NA have been shown to be broadly protective and bind all NAs[27]. In humans, NAI activity has been found to be an independent correlate of protection and the only influence on reduced illness in infected persons[28]. Similar results have been found in a human challenge experiment[29].

Apart from neuraminidase inhibition, NA-binding antibodies can be effective in several ways. During influenza infection of a host cell, NA molecules are presented on the cellular surface. The cell can get opsonized and killed via antibody-dependent cellular cytotoxicity (ADCC) and antibody-dependent phagocytosis (ADCP)[30]. Apart from this obvious mechanism, HA has been found to bind sialic acid on effector cells and therefore increase ADCC[31]. It is hypothesized that NA interferes with this phenomenon by cleaving these sialic acids. This claim is supported by an increase in ADCC activity of anti-HA antibodies by inhibiting NA[31]. Finally, $CD8^+$ cells can probably kill cells displaying linear NA epitopes on MHC I.

Based on that body of evidence, a vaccine that induces anti-NA immunity seems promising. Currently available seasonal influenza vaccines induce a feeble immune response against NA. Only 1-2% of the induced plasmablasts after IIV vaccination are NA specific compared to 14-35% after H3N2 or H1N1 infection [11]. The immunodominance of HA over NA can be partly explained by different stalk lengths and unequal promoter strengths. A switch of the packaging signals of NA and HA, which contain the promoter regions, resulted in virions with higher NA than HA content [32]. By formulating this virus strain into a formaldehyde inactivated vaccine, a stronger immune response of NA targeting Abs compared to the wildtype virus was measured. Adding recombinant NA to QIV could show similar effects. Another work extended the stalk domain of NA by 30 amino acids (AA) to surpass HA [33]. Likely, this resulted in better accessible epitopes which are probably broader effective. By testing the resulting vaccine in mice, a higher titer of Abs using ADCC was measured. A benefit of extending the stalk over the rewiring approach is the unvarying response against HA. Future whole inactivated vaccines, like the QIV could combine both approaches.

Virus-like particles (VLPs) are a vaccine platform which appeared to be effective and subtype cross-protective at the preclinical stage for multiple times targeting NA. Ferrets vaccinated with an N1-NA VLP with a NA derived from a H5N1 strain showed protection against H5N1 challenge [34]. On the contrary, ferrets vaccinated with an N2 VLP showed no protection against H5N1. However, mice vaccinated with an NA-VLP of the 2009 pandemic H1N1 strain were protected against deadly challenge with an H5N1 which shows protection within a subtype but no subtype cross-protection [35].

Recently, progress was made in the field of NA targeting recombinant protein vaccines. Saelens et al. fused broadly protective epitopes of different N1 strains ranging from the 2009 pandemic virus as well as strains dating back to 1933 in one N1 protein [36]. The resulting vaccine showed broad protectiveness against challenge with several N1 viruses. However, the problem of NA instability remains with this platform.

1.4. Conjugation of stabilized neuraminidase to alum

One way to increase the immunogenicity of vaccines is the use of adjuvants. In this work, antigen was conjugated to alum in order to increase its immunogenicity. alum as an adjuvant has been known and used for many decades and is still the most used adjuvant in non-life vaccines. Due to its long-term use, it has an excellent safety profile. It works through several mechanisms of action. On the one hand it activates NLRP3 and PI3 kinase, promotes the release of endogenous danger signals and induces cell death[37]. On the other hand, a working mechanism is the adsorption of the antigen through hydrophobic, electrostatic and ligand exchange mechanisms. This leads to a depot effect. The adsorption can be influenced by using $Al(OH)_3$ (positively charged) or $Al(PO_4)$ (negatively charged) depending on the isoelectric point (pI) of the antigen[38]. In this work, pSer technology is used to further increase antigen binding to alum through ligand exchange[39]. A N-terminal cysteine has been added to the used neuraminidase constructs. The free thiol group reacts covalently with the maleimide end of a linker. The linker consists of maleimide, polyethylene glycol (PEG) and four phosphoserine residues. When added to $Al(OH)_3$ the phosphate residues of the linker replace hydroxide groups of alum and attach the antigen in a stable manner[39]. These particles show superior immunogenicity compared to conventional antigen-alum formulations. An increased induction of germinal centers, neutralizing antibodies, long-lived plasma cells and memory B cells has been shown[39]. Recently, this strategy has been used for the development of an RBD based vaccine against SARS-CoV-2[40].

1.5. Saponin/MPLA Nanoparticles

Saponins are components of the bark of the *Quillaja Saponaria* tree which are in the spotlight of adjuvant research. The name saponin is derived from the word *soap*, since this was their main use until recently[41]. The triterpene glycosides are toxic when injected as free molecules but safe when administered as self-assembled particles together with cholesterol and lipids. The first licensed adjuvant containing saponins was AS01 from the pharmaceutical company GSK. It contains liposomal saponin together with the TLR4 agonist monophosphoryl lipid A (MPLA). This adjuvant has been licensed in vaccines that need a T cell response: Shingrix (a vaccine against shingles) and Mosquirix (a vaccine against malaria)[42,43]. Another formulation of saponins are immune stimulating complexes (ISCOMs). These are nanoparticles with a diameter of around 40 nm that are generated through the self-assembly of saponins, phospholipids and cholesterol. Through their cage-like nature antigen can be incorporated (the ISCOM serves in this case as a transport vehicle) or co-administered. However, the incorporation has not appeared to be beneficial[44]. A SARS-CoV-2 vaccine by the pharmaceutical company Novavax was recently licensed with an ISCOM adjuvant[45]. Due to strong synergistic effects between saponins and TLR4 agonists, MPLA has been incorporated into ISCOMs which led to the adjuvant used in this work: saponin/MPLA nanoparticles (SMNPs). Compared to conventional ISCOMs, SMNP induces 10-to-100-fold higher levels of IFN-α, IFN-γ, IL-6 and TNF-α. This potent activation of the innate immune system has been shown to induce higher germinal center responses and antibody titers against MD39 (a low

immunogenic HIV protein) than AS01, conventional ISCOMs, AddaVax, MPLA and alum[43]. As a reason for this result a potent antigen uptake and enhanced activation and proliferation of B cells is hypothesized to play a roll. As well as an Th1 skewed antiviral functionality profile. The adjuvant is able to enhance lymph flow and therefore increases the antigen delivery to the draining lymph nodes which is necessary for antibodies with somatic hypermutation.

The aim of this work is to test SMNP together with NAs conjugated to alum using pSer technology to investigate a novel influenza vaccine.

2. Methods

2.1. Cells and media

Madin-Darby canine kidney (MDCK) cells (ATCC CCL-34) are epithelial cells derived from the kidney tissue of an adult female cocker spaniel[46]. The cells were passaged in Dulbecco's modified Eagle's medium (DMEM; Gibco) supplemented with 10% (vol/vol) fetal bovine serum (FBS; Gibco) and 1% Penicillin/Streptomycin mix (Pen-Strep; Gibco) that corresponds to 100 U/ml penicillin-100 µg/ml streptomycin. Sf9 cells (*Spodoptera frugiperda*) were passaged in Trichoplusia ni medium – Fred Hink (TNM-FH: Gemini Bioproducts) containing 10 % FBS, 1% Pluronic F-68 (Sigma Aldrich), and. 1% Pen-Strep. For propagation of the baculovirus stocks, TNM-FH media containing 3% FBS, 1% Pluronic F-68 (Sigma Aldrich), and. 1% Pen-Strep was used. High Five cells were kept in SF900 serum, and protein free media supplemented with 1% Pen-Strep.

2.2. Recombinant protein expression

Recombinant proteins were expressed as described previously[47,48]. Briefly, a construct consisting of a gp67 secretion peptide followed by a cysteine (for coupling strategy, described below), a hexahistidine tag, a measles phosphoprotein tetramerization domain, and the head globular domain of either N1 from A/Michigan/45/15 (pSer-N1), N2 from A/Kansas/14/17 (pSer-N2)) or NB from B/Colorado/6/17 (pSer-NB) were cloned into a pFastBac vector. The constructs N1-MPP, N2-MPP and NB-MPP administered with AddaVax share the sequence with pSer-N1, pSer-N2 and pSer-NB only missing the N-terminal cysteine of the pSer constructs that is necessary for coupling with the PEG-linker. The NAs used for ELISAs: Colorado17-NB (B/Colorado/6/17), Michigan15-N1 (A/Michigan/45/15), Kansas17-N2 (A/Kansas/14/17), Phuket13-NB (B/Phuket/307/2013) and Vietnam04-N1 (A/Vietnam/1204/2004) were expressed with a vasodilator stimulating phosphoprotein (VASP) tetramerization domain in order to measure only NA-ectodomain specific antibodies. The plasmids were transformed into DH10Bac, a bacteria strain allowing recombination between pFastBac and the baculovirus shuttle vector bMON14272. Recombinant clones were selected using blue-white screening, midipreped, and transfected into Sf9 cells (*Spodoptera frugiperda* derived) for baculovirus rescue. Recombinant baculovirus was propagated in Sf9 cells and used for protein production in High Five cells (BTI-TN-5B1-4 cells derived from *Trichoplusia ni*) at a multiplicity of infection (MOI) of 10. High five cells were incubated for 3 days at room temperature as suspension cells in shake flasks. Cells were separated using low-speed centrifugation and the supernatant was mixed with Ni^{2+} resin. The resin was captured in filter columns and washed. The proteins of interest were eluted using an imidazole-containing buffer and diafiltrated against PBS using centrifugation units (30 kDa MWCO). Aliquoted protein in PBS was stored at -80°C.

2.3. Adjuvants

The SMNP adjuvant was prepared by collaborators as previously described [43,49]. Briefly, cholesterol (20 mg/ml; Avanti Polar Lipids), MPLA (Avanti Polar Lipids) DPPC (1,2-dipalmitoyl-sn-glycero-3-phosphocholine, 20 mg/ml, Avanti Polar Lipids) were mixed separately with Milli-Q water containing 20% (w/v) MEGA-10 (Sigma Aldrich) at 60°C. Quil-A saponin (InvivoGen) was dissolved in Milli-Q water and mixed with the other components at a molar ratio of 10:10:2.5:1 (Quil-A:cholesterol:DPPC:MPLA). The solution was diluted to 1mg/ml cholesterol and incubated at 25°C overnight to allow self-assembly. Non-assembled precursors were

removed by dialysis against PBS with a 10k MWCO membrane and SMNPs sterile filtered using a 0.2 µm Supor syringe filter. The remaining solution was further concentrated with a 50k MWCO filter and polished with a Sephacryl S-500 HR size exclusion column. For quality control, each batch was characterized by negative stain transmission electron microscopy (TEM), dynamic light scattering (DLS) for structural integrity and uniform size. Endotoxin content was monitored using a Limulus Amebocyte Lysate assay (Lonza). Assuming a stoichiometric incorporation of all precursors the final adjuvant concentration was measured by determination of the cholesterol content (Cholesterol Quantitation Kit; MilliporeSigma).

Conjugation to alum was done as previously described by collaborators[39,40]. Neuraminidase constructs with free N-terminal cysteine residues (pSer-N1, pSer-N2 and pSer-NB) were reduced at 1 mg/ml with 2 times the molar amount of tris(2-carboxyethyl)phosphine (TCEP; Thermo Fisher Scientific) at 25°C for 10 minutes. TCEP, the reducing reagent, was removed by 10k MWCO centrifugal filters. Subsequently, the reduced antigen was allowed to react with pSer-maleimide linkers for 16 hours in tris-buffered saline (TBS). Remaining pSer linker was removed with a 10k MWCO membrane and the buffer exchanged to PBS.

Before vaccination, the conjugated constructs were incubated with the corresponding alum amount for 30 minutes. Then, the remaining PBS and SMNP was added.

The NA constructs without an N-terminal cysteine residue (N1-MPP, N2-MPP and NB-MPP) were diluted in PBS to the desired concentration and incubated with AddaVax (InvivoGen) for 30 minutes. Amounts of adjuvant used are depicted in Table 1.

2.4. Challenge viruses

2.4.1. Influenza A viruses

A/Singapore/GP1908/2015 (H1N1) was used as part of the influenza vaccine in Japan for the seasons 2017/2018 and 2018/2019 [50]. The strain used here as a challenge virus consists of the internal proteins of A/Texas/1/77 (H3N2) and the surface glycoproteins of A/Singapore/GP1908/2015. A/Vietnam/1204/2004 (H5N1) was initially isolated during one of the largest and most lethal H5N1 outbreaks until now [51]. The strain used here possesses the internal proteins of A/Puerto Rico/8/34 (H1N1) and the outside glycoproteins of A/Vietnam/1203/04. Additionally, the H5 lacks its polybasic cleavage side. The challenge strain A/Switzerland/9715293/13 (H3N2) is mouse-adapted and possesses its natural internal proteins. All influenza A virus stocks were propagated in 10-day-old embryonated chicken eggs. The respective virus solution was injected into the allantoic cavity of the embryonated egg, following a 48 hour incubation period at 37°C. The allantoic fluid was harvested after incubation for 3 days at 33°C, centrifuged at 1000x*g* for 10 minutes at 4°C, sterile filtered, aliquoted, and frozen at -80°C.

2.4.2. Influenza B viruses

B/New York/PV01181/2018 represents the Victoria lineage, and B/New York/PV00094/2017 the Yamagata lineage. Both were isolated by the Personalized Virology Initiative at Icahn School of Medicine at Mount Sinai[52]. Both were mouse-adapted. B/New York/PV00094/2017 (Yamagata) loses its virulence when propagated in eggs. Therefore, three 12-week-old mice (Jackson Laboratories) were inoculated with 50 µl of neat virus stock. After 48 hours, the mice were euthanized by cervical dislocation, and the lungs homogenized (Beadblaster 24, Benchmark) with 3 mm Zirconium beads in 500 µl PBS. After centrifugation (260x*g* for 10 minutes at 4°C), the supernatant was aliquoted, and the titer was determined via plaque assay

(described below).
B/New York/PV01181/2018 (Victoria) can be passaged alternating in eggs and mouse lungs. Therefore, the stock solution derived from eggs was first passaged in a mouse - similarly to the B/New York/PV00094/2017 strain. The virus solution derived from the mouse lungs was diluted at 1:1000 and injected into the allantoic cavity of 10-day-old embryonated chicken eggs. After an incubation 72 hours at 33°C the allantoic fluid was harvested similar as described above for influenza A.

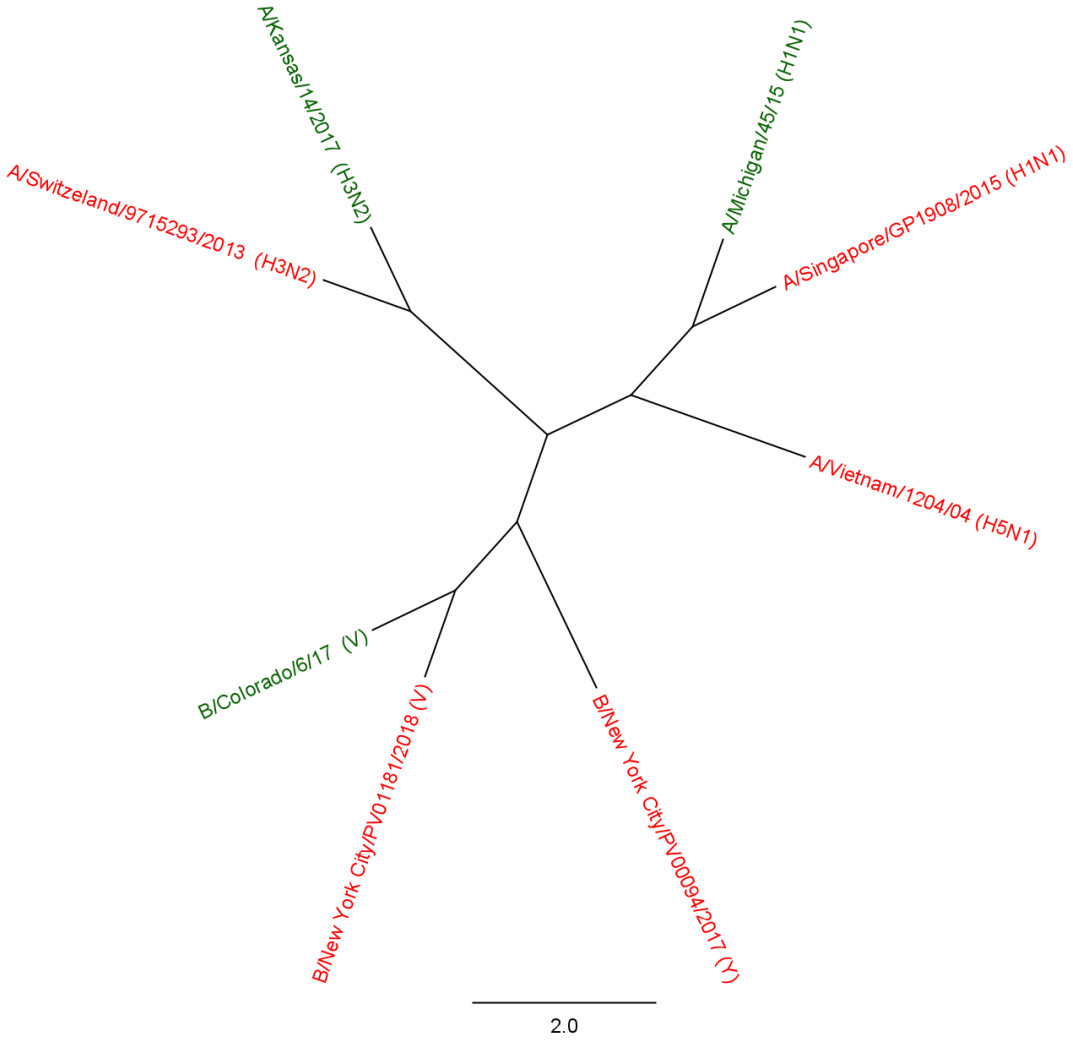

Figure 1 Neuraminidase amino acid-based cladogram of vaccine (in green) and challenge strains (in red). Tree built in Geneious Prime 11. Based on a global alignment with free ends and gaps. Tree built with the Jukes-Cantor model without an outgroup.

2.5. Hemagglutination assay

The hemagglutination assay was performed as described elsewhere[53]. Briefly, allantoic fluid from each egg was diluted 1:2 in PBS on a 96 well V-bottom plate. Turkey red blood cells (RBCs) were washed with PBS and diluted to 0.5%. 50 µl of the RBCs were added to 50 µl of the virus dilutions. The plate was incubated at 4°C for 45 min. HA activity crosslinks red blood

cells and keeps them from settling. Therefore, a cloudy well indicates HA activity, precipitated red blood cells indicate no HA activity and therefore no virus.

2.6. Plaque assay

To determine the titers of the generated virus stocks, plaque assays on MDCK cell monolayers were done as previously described[26,54]. Briefly, 4 x 10^5 MDCK cells per well were plated the day before performing the assay in 12-well plates in cDMEM. Virus stocks were diluted 10-fold to a 10^{-6} dilution and incubated with occasional rocking for 1 h at 37° C or 33° C respectively. After the infection, the fluid was removed and replaced by an agarose overlay containing a final concentration of 10% 10× minimal essential medium (MEM, Gibco), 2 mM L-glutamine (Gibco), 0.1% of sodium hydrogen carbonate (Gibco), 10 mM 4-HEPES, 100 U/ml penicillin–100 µ/ml streptomycin, and 0.2% bovine serum albumin (BSA), 1 µ/ml TPCK (tolylsulfonyl phenylalanyl chloromethyl ketone)-treated trypsin, 0.64% agarose (Oxoid), and 0.1% (wt/vol) DEAE (diethylaminoethyl)-dextran. Plates were incubated for 2 days at 37°C (influenza A) or 3 days at 33°C (influenza B). After the incubation period, the cells were fixed using 10% formaldehyde and the plaques visualized with a crystal violet counterstain (Sigma-Aldrich).

2.7. ELISA

96-well microtiter plates (Immulon 4 HBX plates, ThermoFisher) were coated overnight with 50 µl of 2 µg/ml of recombinant VASP-NA in PBS. The plates were subsequently washed on an automated plate washer and blocked with 100 µl of blocking solution containing 0.5% dry milk powder (RPI), 3% goat serum (Gibco) and 96.5 % PBS-T (0.1% Tween 20 (Fisher BioReagents) and 99.9% PBS pH=7.4) for 1 hour. After removal of the blocking solution the plates were incubated for 2 hours at RT with serum diluted initially 1:50 and then serially diluted 1:3 in blocking solution. After incubation the plates were washed 3 times with PBS-T using an automated plate washer (BioTek 405TS microplate washer). As a secondary antibody either anti-mouse-IgG, anti-mouse-IgG2a, or anti-mouse-IgG1 was used. All secondary antibodies are horseradish peroxidase conjugated. The secondary antibodies were diluted in blocking solution and incubated on the plates for one hour. Subsequently, the plates were washed 3 times with PBS-T using the automated plate washer and 100 µl SigmaFast o-phenylenediamine dihydrochloride (Sigmafast OPD; Sigma-Aldrich) was added. After 10 minutes of incubation the reaction was stopped by adding 50 µl of 3 mol/l HCl and optical density was measured at a wavelength of 490 nm using a plate reader (BioTek, SYNERGY H1 microplate reader). The area under the curve (AUC) values were calculated with a cutoff of 5 times the mean signal of the serum free wells and plotted using Prism 9 (GraphPad).

2.8. Neuraminidase inhibition (NI) assay

96-well microtiter plates (Immulon 4 HBX plates, ThermoFisher) were coated overnight with 100 µL of 50 µg/mL fetuin (Sigma-Aldrich) at 4°C overnight and washed 3 times with PBS-T on an on an automated plate washer (BioTek 405TS microplate washer). Serum samples were inactivated for 1 hour at 56°C and diluted 1:50 in PBS and further 1:2 serially diluted on a fresh 96 well plate. 50 µl of the diluted serum were added to the respective wells of the fetuin coated plate. Either 50 µl of A/Singapore/GP1908/2015, A/Kansas/14/17, A/Vietnam/1204/2004, B/New York/PV00094/2017, or B/New York/PV01181/2018 were added to the sera at 2 times the 50% effective concentration (EC_{50}). EC_{50} values were determined with the same procedure, only without serum. The virus-serum mixture was incubated on the fetuin coated plates for 16-18 hours at 37°C (influenza A) or 33°C (influenza B). After the incubation time,

the plates were washed 3 times with PBS-T on an automated plate washer. The amount of free galactose residues was determined by adding 100 µl/well of peanut agglutinin conjugated to horseradish peroxidase (HRP) (PNA 5 µg/ml; Sigma Aldrich) for 2 h at RT. After washing the plates 3 times with PBS-T on an automated plate washer 100 µl SigmaFast o-phenylenediamine dihydrochloride (Sigmafast OPD; Sigma-Aldrich) was added. The reaction was stopped by adding 50 µl of 3 mol/l HCl after 10 minutes. Optical density was measured at 490 nm using an automated plate reader (BioTek, SYNERGY H1 microplate reader). OD values were normalized using virus free wells as lowest signal and serum free virus only wells as highest signal. ED_{50} values were calculated fitting a four-parameter logistic curve in Prism 9 (GraphPad).

2.9. Animal work

For all animal immunizations 6- to 8-week-old female BALB/c mice (challenged with A/Singapore/GP1908/2015, A/Vietnam/1204/2004, B/New York/PV00094/2017, or B/New York/PV01181/2018) or DBA.2 mice (challenged with A/Switzerland/9715293/13) were used (Jackson laboratories). All experiments were conducted under protocols approved by the Icahn School of Medicine at Mount Sinai Institutional Animal Care and Use Committee (IACUC). The different antigen and adjuvant doses are depicted in Table 2: Antigen and adjuvant dose of each group.Table 2.

Table 2: Antigen and adjuvant dose of each group.

Group name	Antigen			Adjuvant		
	pSer-N1 µg	pSer-N2 µg	pSer-NB µg	SMNP µg	alum µg	alum:NA ratio
N1+N2+NB alum low	1	1	1	5	2.25	1:0.7
N1+N2+NB alum high	1	1	1	5	30	1:10
N1 alum low	1	0	0	5	0.7	1:0.7
N1 alum high	1	0	0	5	10	1:10
HIV trimer MD39						
MD39		3		5	10	1:0.7
	N1-MPP µg	N2-MPP µg	NB-MPP µg	AddaVax µl		
N1+N2+NB AddaVax	1	1	1	50		

6–8-week-old female mice were vaccinated subcutaneously at the base of the tail in a prime-boost regime with 4 weeks between prime and boost. Each side of the tail was injected with 100 µl vaccine. 4 weeks after boost mice were challenged intranasally with 50 µl virus dilution as depicted in Figure 2. Weight loss was monitored 14 days post challenge. Mice were culled using cervical dislocation when a weight loss of 25% was reached.

On day 28 blood was taken from the submandibular vein without anaesthesia. On day 56 blood was taken retro-orbitally with anaesthesia. Mice were anaesthetized with an intraperitoneal injection of 0.1 ml of a ketamine/xylazine cocktail (0.15 mg ketamine and 0.03 mg xylazine per mouse). Blood was allowed to clot over night at 4 °C. Subsequently, the blood was centrifuged at 8500x*g* for 10 minutes and the serum harvested.

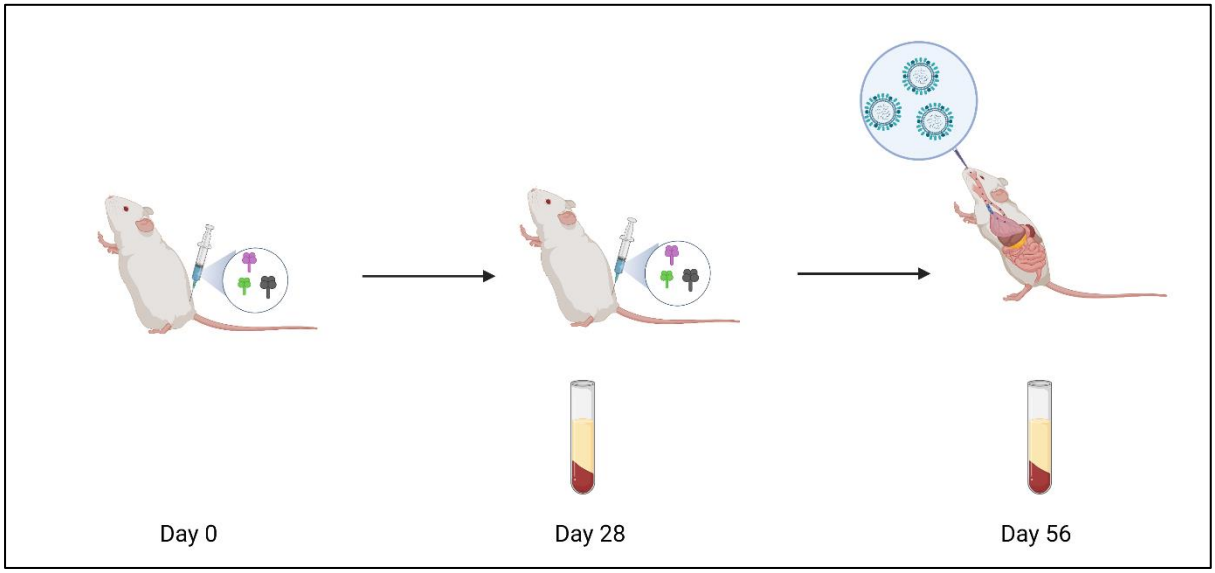

Figure 3 Vaccination, challenge and bleeding regime. Figure created with BioRender.

To determine the half-maximal lethal dosages (LD_{50}) of the virus stocks, 16–18-week-old female BALB/c mice (or DBA.2 mice for A/Switzerland/9715293/13 (H3N2)) were inoculated with 50 µl of different virus dilutions. For each virus 5 1:10 dilutions of virus were tested in groups of N=3 mice. LD_{50}s were calculated in Microsoft Excel using the method of Reed and Muench[55].

2.9 Data analysis

AUC and ED_{50} values were calculated using Prism 9. For the latter, a four-parameter logistic curve was fitted. To choose an appropriate test to compare antibody titers a Kolmogorov-Smirnov test was done as well as visual examination of the data at Q-Q plots. Kolmogorov-Smirnov test as well as the Q-Q plot failed for some groups. This fact, as well as the small sample size per group (N=5) led to the decision of using the non-parametric Kruskal-Wallice-Test corrected for multiple comparisons with Dunn`s test To correlate antibody titers a linear regression was done. $P<0.05$ was defined as a statistically significant difference. All graphs and statistical tests were done with Prism 9.
To calculate LD_{50}s Microsoft Excel and the Method of Reed and Muench[55] was used. Antibody titers below the limit of detection (LOD) are shown for illustrative purposes as constant values below the LOD.

3. Results

3.1. Immunological evaluation of the vaccine

To assess the effect of the prime-boost vaccination regime, the IgG titers measured via ELISA were compared between day 28 (post-prime) and day 56 (post-boost). Figure 4 shows a noticeable difference for all measured antigens. The difference is in particular notable against the heterologous VNO4-VASP-N1 protein.

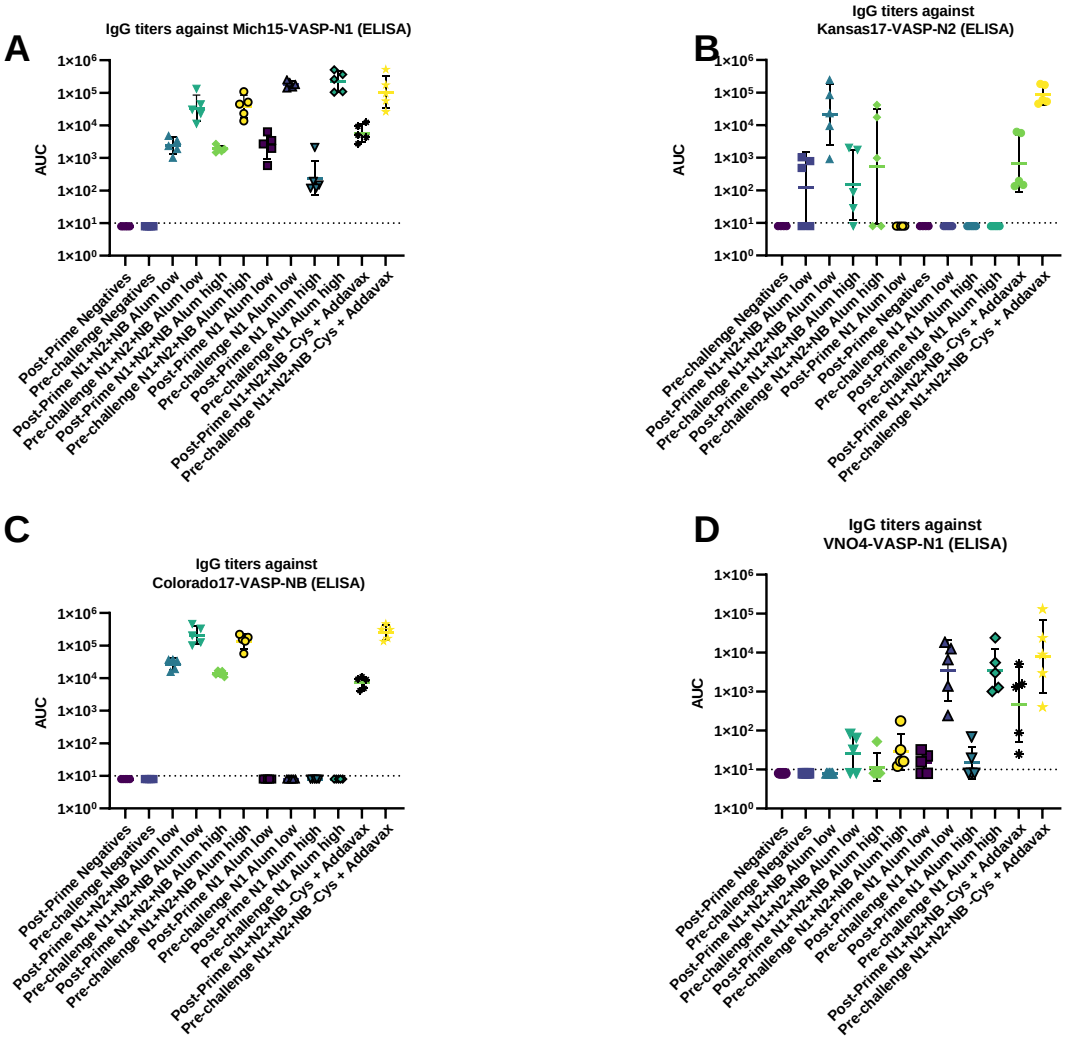

Figure 4 Comparison between ELISA IgG titers Post-Prime and Pre-challenge against **A** Mich15-VASP-N1, **B** Kansas17-VASP-N2, **C** Colorado17-VASP-NB and **D** VNO4-VASP-N1

Figure 5 shows the ratios of IgG1 to IgG2a antibodies elicited against Michigan15-N1 by DBA.2 mice. This ratio serves as a surrogate for an immune response skewed towards Th1-like or a Th2-like T helper cell response. The *alum high* formulations as well as the AddaVax group show a more Th2 like response. The *alum low* groups a more Th1 like response. Nevertheless, the data is very widespread. Therefore, only trends can be derived from Figure 5.

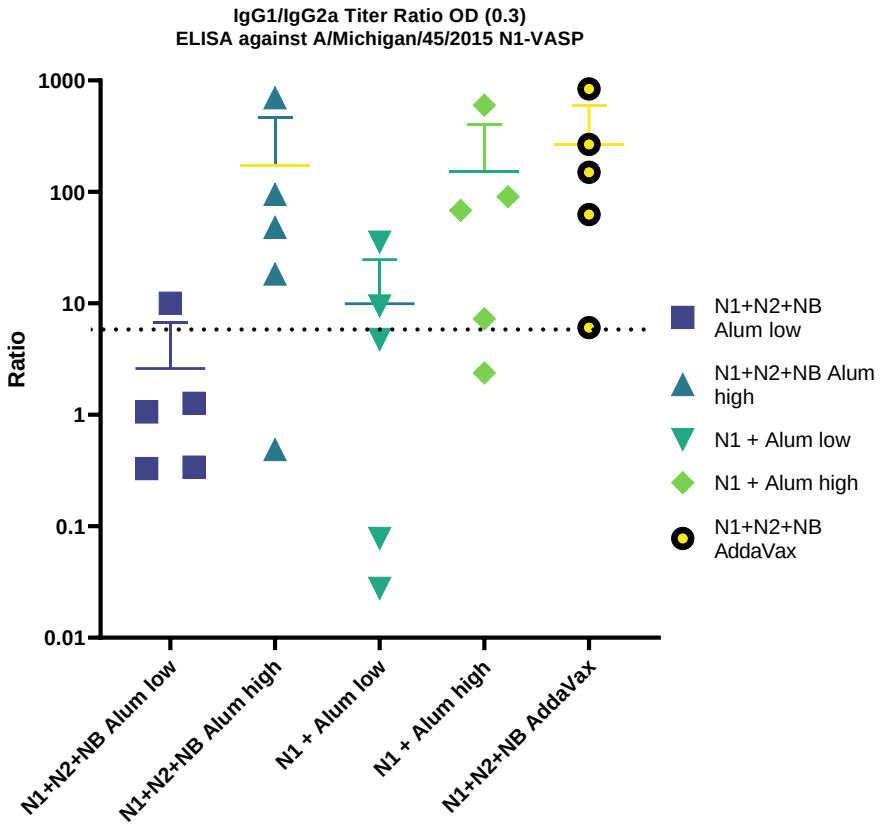

Figure 5 Ratios of IgG1 to IgG2a titers at OD = 0.3. Shown are means ± standard deviation. Titers are measured against Michigan15-VASP-N1. N=5 mice per group.

3.2. Challenge with homologous and heterologous influenza strains

56 days after prime, the mice were challenged with viruses. The different virus doses were chosen depending on the antigenic distance between the NAs in the vaccine and the the challenge virus (Figure 1 shows a cladogram of amino acid similarity of the challenge and vaccine strains as a surrogate for antigenic distance). pH1N1 (A/Singapore/GP1908/2015), H3N2 (A/Switzerland/9715293/2013) and B-Victoria (B/New York/PV01181/2018) represent the homologous challenge of the vaccine. Therefore, 25 xLD_{50} were used as a challenge dose. B-Yamagata (B/New York/PV00094/2017) and H5N1 serve as heterologous challenge. that B-Yamagata might have become eradicated during the COVID-19 pandemic[56]. This is one of the reasons why it was not included as a vaccine antigen. H5N1 circulates in birds all over the world. Occasional spillovers into humans can be observed. Therefore, a H5N1 pandemic is possible and would could have a large impact due to its high case fatality rate of around 50%[51,57].
Figure 6, Figure 7, Figure 9, Figure 10, and Figure 11 show weight loss and survival after challenge as well as a humoral immunity profile of the challenged mice in form of binding antibody titers measured via ELISA and functional antibody titers measured via NAI assay.

Figure 6A shows the weight loss after challenge with 25 xLD_{50} of A/Singapore/GP1908/2015. The mice adjuvanted with AddaVax show except day 3 no weight loss which makes them to the best performing group. Day 3 can be interpreted as an outlier since day 2 and 4 show no weight loss at all. The mice vaccinated with the control protein MD39 all die on day 5. Temporal weight loss can be observed for all other groups. Group *N1+N2+NB alum low* shows the most weight loss. This is supported by lower levels of NAI antibodies as seen in Figure 6D. Figure 6C shows lower binding antibody titers for the trivalent vaccine formulations. The monovalent

groups as well as the AddaVax group show higher titers than the SMNP/alum adjuvanted trivalent groups.

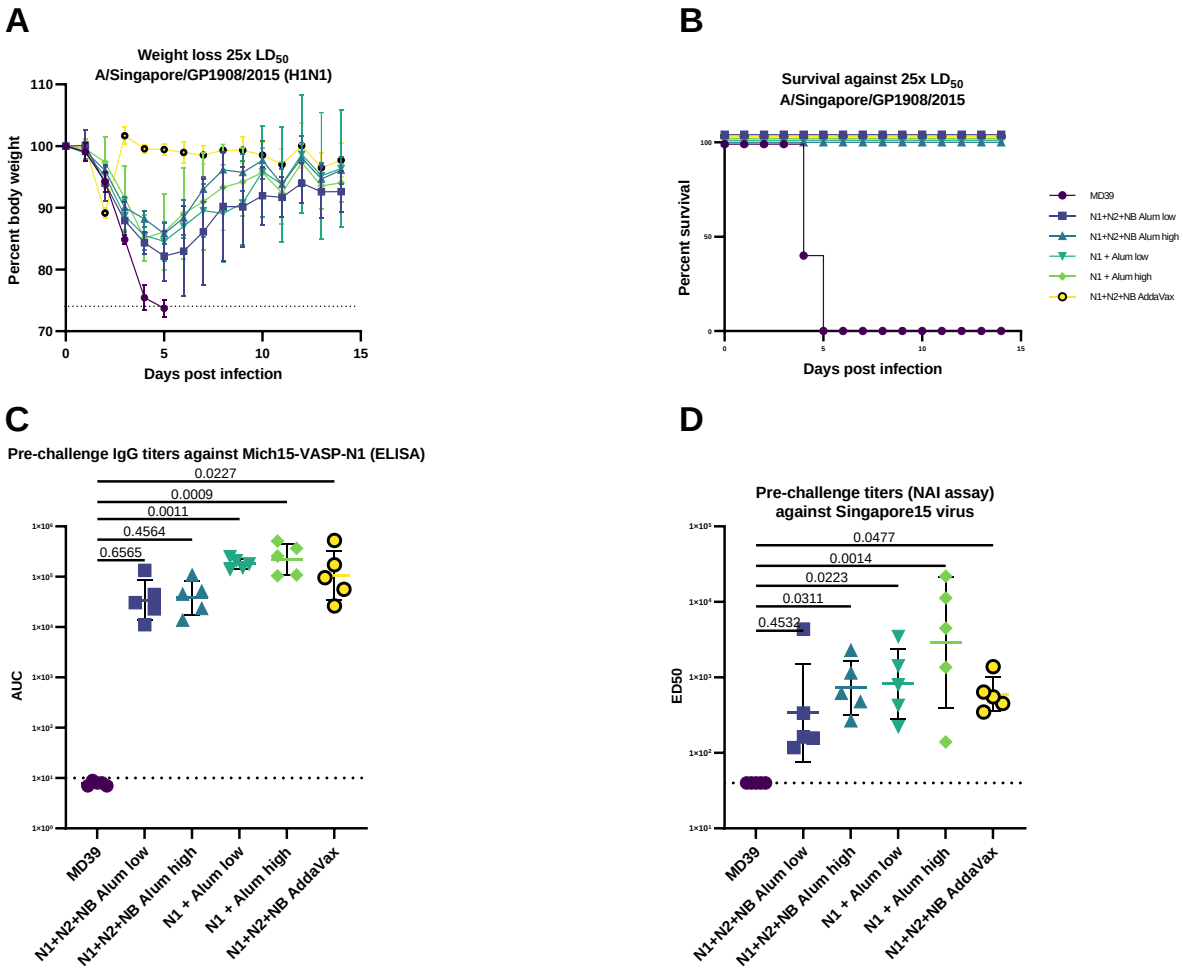

Figure 6 Challenge with 25x LD_{50} A/Singapore/GP1908/2015 (H1N1). **A** Weight loss curve. Shown are means ± standard deviation. **B** Survival after challenge. **C** Pre-challenge IgG titers against Mich15-VASP-N1 measured via ELISA. Geometric means ± geometric standard deviations are shown. **D** Pre-challenge NAI titers against the challenge strain A/Singapore/GP1908/2015. Shown are geometric means ± geometric standard deviation. Statistical analysis in **C** and **D** was done using a Kruskal-Wallice-Test corrected for multiple comparisons with Dunn`s test. N=5 per group in **A**, **B**, **C** and **D**

Figure 7A shows the weight loss after challenge with 25 xLD_{50} of A/Switzerland/9715293/2013 (H3N2). All groups without N2 in the vaccine were dead by day 9. Group *N1+N2+NB alum low* showed the least weight loss. Only 1 out of 5 mice died in the groups *N1+N2+NB alum low* and *N1+N2+NB AddaVax*. The ELISA and NAI titers show a very heterogenous immune response. The titers of 2 mice of *N1+N2+NB alum high* were not even detectable with the ELISA. These mice did not survive the challenge.

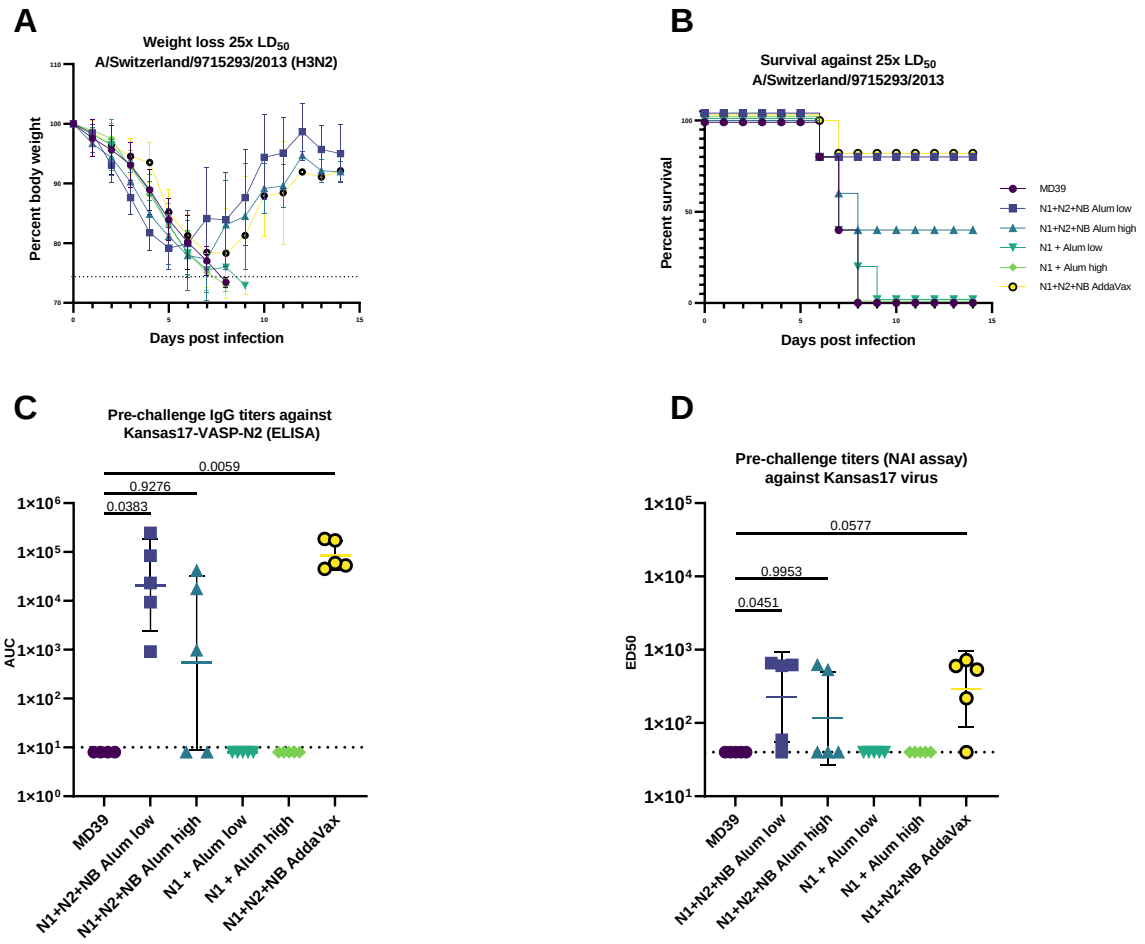

Figure 7 Challenge with 25x LD50 A/Switzerland/9715293/2013 (H3N2). **A** Weight loss curve. Shown are means ± standard deviation. **B** Survival after challenge. **C** Pre-challenge IgG titers against Kansas17-VASP-N1 measured via ELISA. Geometric means ± geometric standard deviations are shown. **D** Pre-challenge NAI titers against the vaccine strain A/Singapore/GP1908/2015. Shown are geometric means ± geometric standard deviation. Statistical analysis in **C** and **D** was done using a Kruskal-Wallice-Test corrected for multiple comparisons with Dunn`s test. N=5 per group in **A**, **B**, **C** and **D**

To see if the heterogenous immunogenicity is specific to N2, the titers against Michigan15-N1 and Kansas 17-N2 have been correlated in Figure 8. Antigen binding titers correlate significantly (R^2=0.6, p=0.006). The 2 mice showing no response against N2 reacted also poorly to N1. Taken together, it seems as if the vaccination of some of the mice challenged with A/Switzerland/9715293/2013 (H3N2) was not successful. Therefore, it is hard to derive conclusions from this challenge.

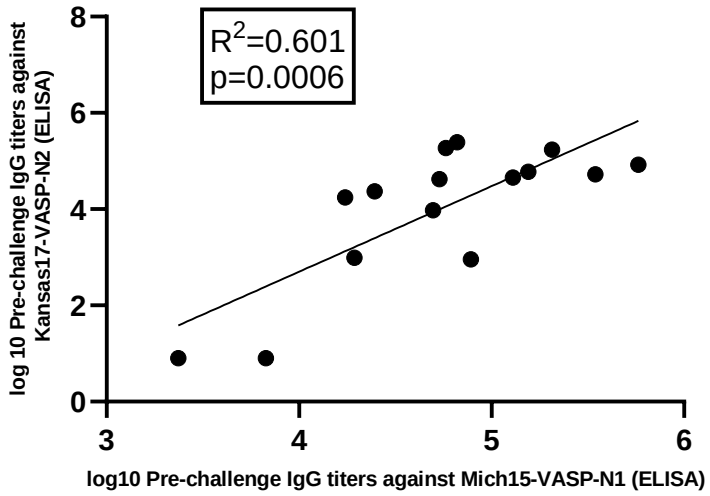

Figure 8 Correlation of ELISA titers against Mich15-VASP-N1 and Kansas17-VASP-N2 of the mice challenged with A/Switzerland/9715293/13 (H3N2) . Statistical analysis was done using a linear regression.

Figure 9B shows that 4 out of mice vaccinated with monovalent formulations survived. All mice vaccinated with a trivalent formulation died except one mouse in the *N1+N2+NB alum high* group. According to Figure 9A, the group *N1 alum low* showed the least weight loss. NAI titers against A/Vietnam/1203/2004 were either not elicited or below the limit of detection. The binding antibody titers in Figure 9C show, consisting with survival and weight loss data, high titers for the monovalent groups. Contradicting to the information provided by Figure 9A and Figure 9B, the group adjuvanted with AddaVax also showed high binding titers to Vietnam04-N1.

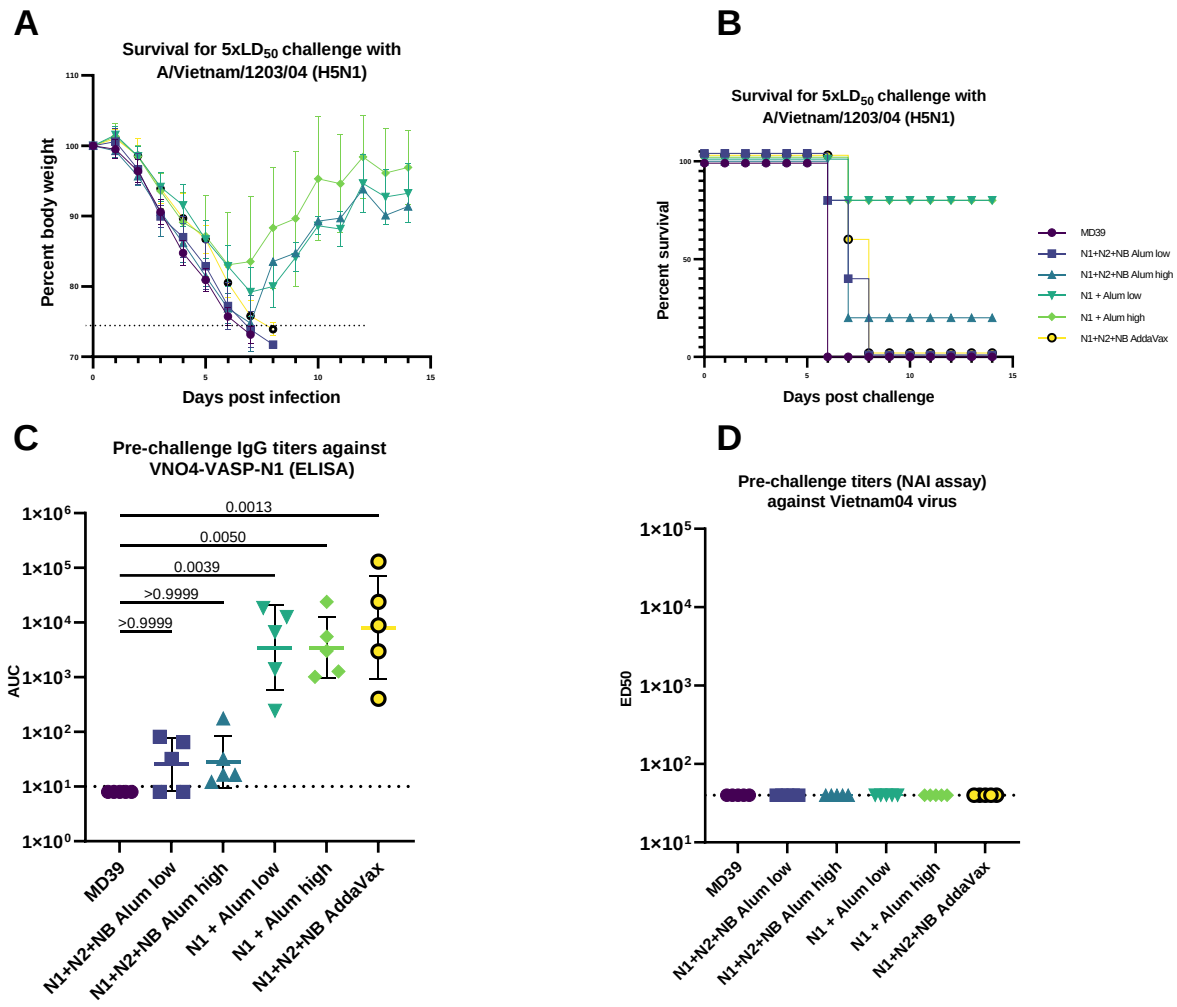

Figure 9 Heterologous challenge with 5x LD50 A/Vietnam/1203/2004 (H5N1). **A** Weight loss curve. Shown are means ± standard deviation. **B** Survival after challenge. **C** Pre-challenge IgG titers against VNO4-VASP-N1 measured via ELISA. Geometric means ± geometric standard deviations are shown. **D** Pre-challenge NAI titers against the challenge strain A/Vietnam/1203/2004. Statistical analysis in **C** was done using a Kruskal-Wallice-Test corrected for multiple comparisons with Dunn`s test. N=5 per group in **A**, **B**, **C** and **D**

Figure 10B shows that every group without being vaccinated with an NB containing vaccine died at day 6 the latest after challenge with 25 xLD_{50} B/New York/PV01181/2018 (Victoria). The other groups show very little but equal weight loss as seen in Figure 10A. This corresponds to very similar functional as well as binding titers between the groups as seen in Figure 10C and D.

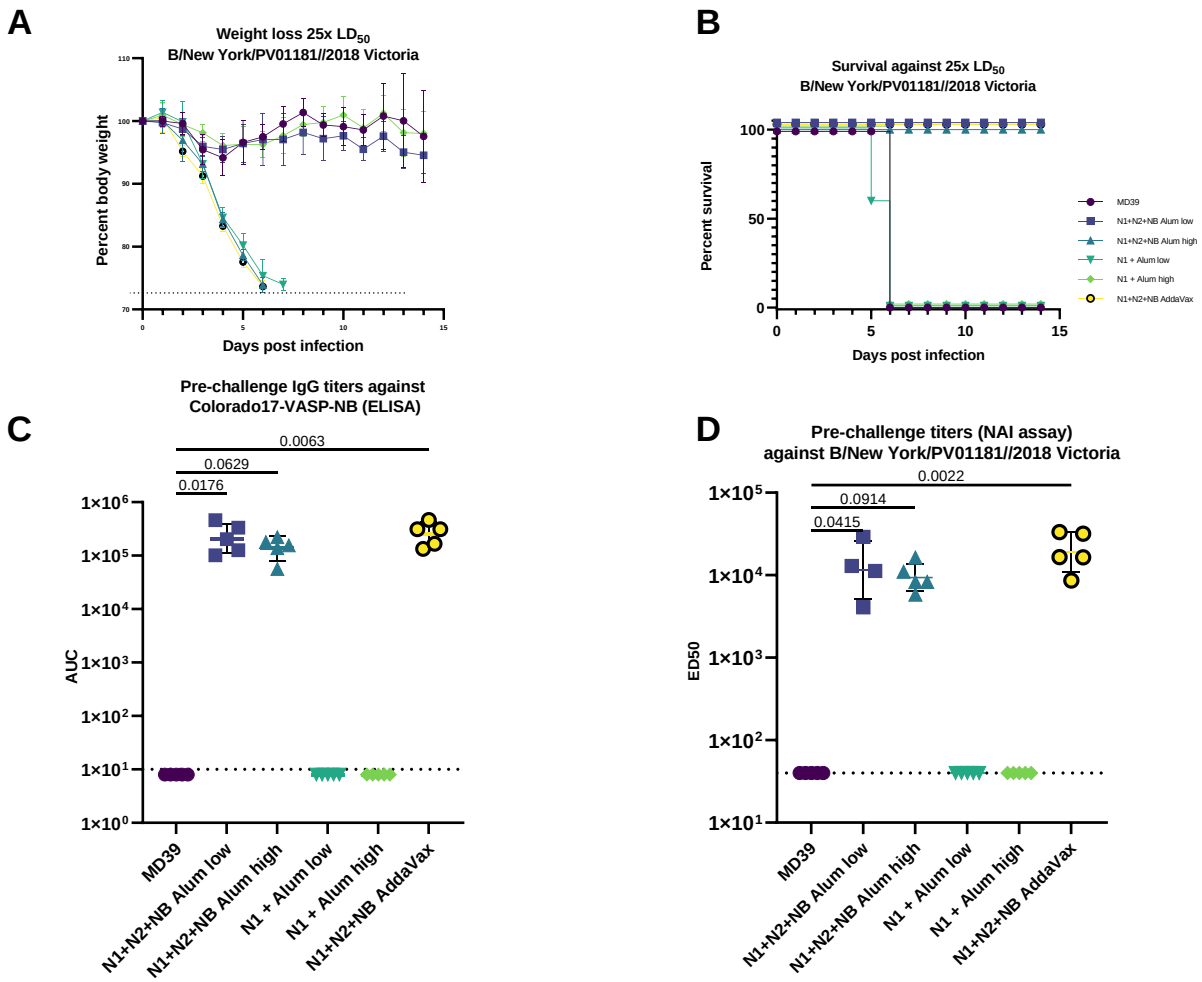

Figure 10 Challenge with 25x LD50 B/New York/PV01181/2018 (Victoria). **A** Weight loss curve. Shown are means ± standard deviation. **B** Survival after challenge. **C** Pre-challenge IgG titers against Colorado17-VASP-NB measured via ELISA. Geometric means ± geometric standard deviations are shown. **D** Pre-challenge NAI titers against the vaccine strain B/New York/PV01181/2018. Shown are geometric means ± geometric standard deviation. Statistical analysis in **C** and **D** was done using a Kruskal-Wallice-Test corrected for multiple comparisons with Dunn`s test. N=5 per group in **A**, **B**, **C** and **D**

The challenge with 5x LD50 B/New York/PV00094/2017 (Yamagata) was the only challenge with negative control animals surviving as seen in Figure 11. 3 out of 5 animals died in the negative control group *MD39 as well as in N1 + alum high*. 2 out of 5 animals died in *N1 + alum low*. All mice that were vaccinated with an NB protein survived. Interestingly, the *N1+N2+NB alum high* group showed less weight loss than *N1+N2+NB alum low* which is a contradicting finding compared to the other challenges. Since, B/New York/PV00094/2017 (Yamagata) is distant to the vaccine protein Colorado17-NB, no binding or functional antibodies could be detected.

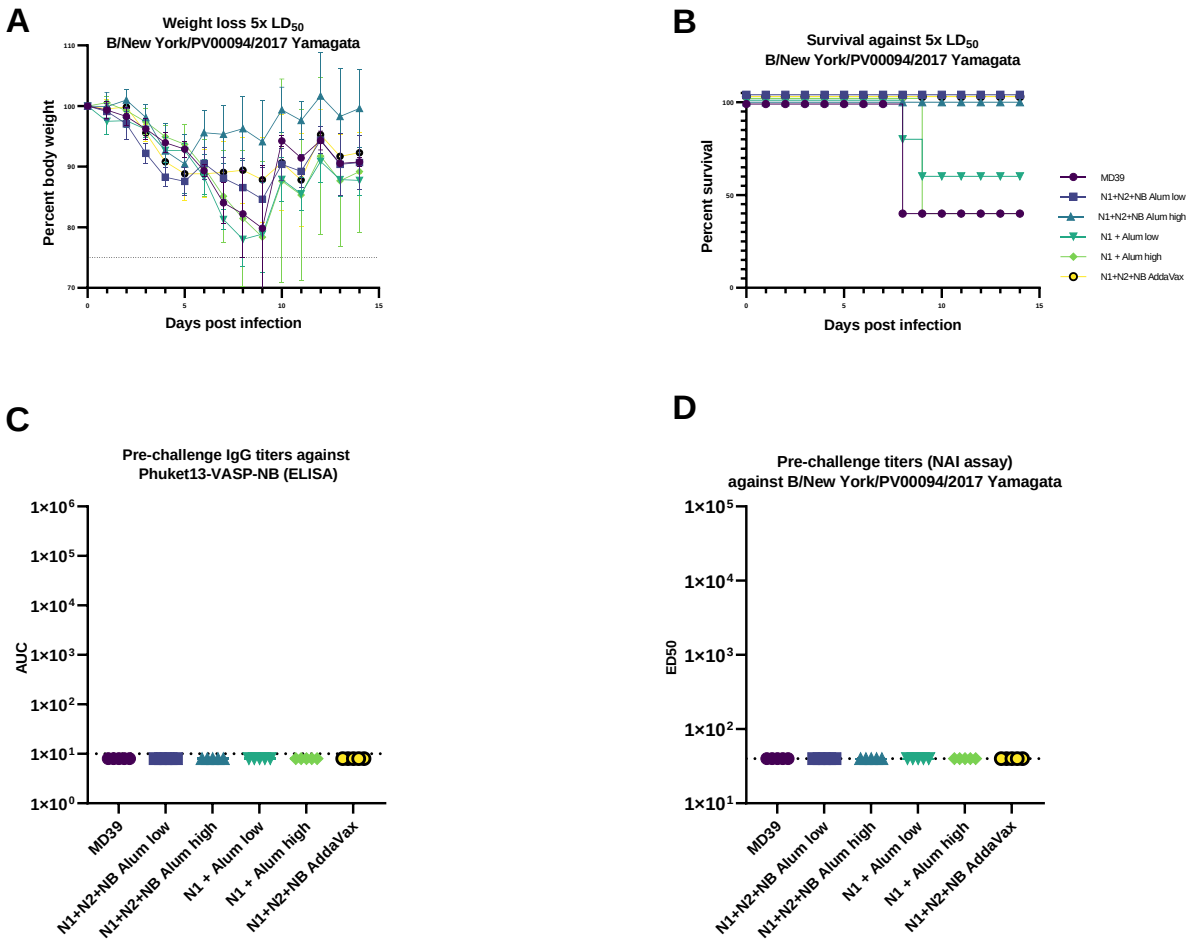

Figure 11 Challenge with 5x LD50 B/New York/PV00094/2017 (Yamagata). **A** Weight loss curve. Shown are means ± standard deviation. **B** Survival after challenge. **C** Pre-challenge IgG titers against Phuket13-VASP-NB measured via ELISA. **D** Pre-challenge NAI titers against the vaccine strain B/New York/PV01181/2018. N=5 per group in **A**, **B**, **C** and **D**

4. Discussion

Pandemic influenza circulates in humans since approximately 500 years[58]. Until now, its seasonal burden and pandemic potential remain a constant threat. This work aims to take a step towards mitigating this problem.

The evaluation of the humoral immunity revealed the need for 2 doses. Figure 4This aligns with previous work showing a similar effect with the CpG 1018 adjuvant[59]. This would be different in adult humans that already have been primed with NA. For this group, one shot is probably sufficient. If the vaccine was delivered to human newborns, 2 doses would be required.
The difference between the post-prime and pre-boost titers against Vietnam-N1 is larger than for the homologous antigens. This could result from the induction of germinal centers and somatic hypermutation. AddaVax[60], antigen coupled to alum with the pSer technology[39] and SMNP[43] have independently shown their ability to induce germinal centers. However, the data obtained is not sufficient to confirm or disprove this theory.

The measured IgG_1/IgG_{2a} ratio indicates a different T cell polarization induced by different vaccine formulations. In general, naïve B cells reside in lymph nodes until they encounter an antigen. This triggers the migration to the outer T-cell zone of the lymph nodes[61]. There, B cells can be further activated by Dendritic cells or T-cells that enable B-cell differentiation into a short-lived plasma cell. This is called an extrafollicular reaction[62,63]. In mice, Th1 or Th2 T-cell help leads to different kinds of antibodies. IFN-γ-producing Th1 cells promote a class switch towards IgG_{2a}, IL-4 producing Th2 T cells towards IgG_1 (in humans, most antibodies are IgG_1)[63,64]. Th1 like immune responses are associated with intracellular pathogens and Th2 like immune responses with extracellular parasites. Since viruses replicate inside cells, a Th1 like response is usually desired. alum has been shown to skew the immune response towards Th2[37]. The same is true for the oil-in-water adjuvant AddaVax[65]. SMNP, containing the immunomodulators MPLA and saponin has been found to induce Th1 T cell populations[43]. This explains the pattern observable in Figure 5 with Th2 like responses of groups adjuvanted with high alum concentrations or AddaVax and more Th1 like responses in the groups with low alum content in ratio to SMNP (see Table 2).

One of the scopes of this work was to find the best formulation of a trivalent influenza vaccine against death or disease by virus. When challenged with A/Singapore/GP1908/2015 (H1N1) the group challenged with AddaVax showed clearly the smallest weight loss. The trivalent AddaVax group and the monovalent SMNP/alum groups showed the highest antibody titers which does not explain why these groups experienced such big difference in weight loss. After challenged with A/Switzerland/9715293/13 (H3N2) the *N1+N2+NB alum low* group shows the least weight loss and together with the AddaVax group the highest survival. This aligns with binding antibody titers that are high for these two groups. The NAI titers are of similar magnitude for all groups.
The binding antibody titers against Vietnam04-N1 shown in Figure 9C show the highest titers elicited of the trivalent AddaVax group and the monovalent groups. However, all mice in the AddaVax group die while 80% of the mice vaccinated with a monovalent vaccine survive. One can hypothesize that the antibodies elicited by the monovalent SMNP/alum adjuvanted vaccine more functional. Even though this functionality is below the limit of detection of the used NAI assay.
Challenged with B/New York/PV01181/2018 (Victoria) no group vaccinated with NB shows significant weight loss. The antibody titers of the *N1+N2+NB AddaVax* and *N1+N2+NB alum low* are slightly higher than of *N1+N2+NB alum high*. The difference was probably not seen due to in weight loss due to the consistent high titers.
The challenge with B/New York/PV00094/2017 (Yamagata) was the only one with not all control animals dying. Interestingly, the *N1+N2+NB alum high* group showed the least weight

loss. This was the only time this group performed the best. Since ELISA and NAI titers were below the limit of detection, a comparison is not possible.
This data can be compared to a similar vaccine consisting of the same antigens as in the *N1+N2+NB AddaVax* group but adjuvanted with CpG 1018[59]. This vaccine was challenged with A/Singapore/GP1908/2015 (H1N1) and A/Vietnam/1204/2004 (H5N1). Interestingly, in this work antigenic competition was observed as a consistent pattern. Monovalent vaccine formulations performed better than all trivalent ones in the H5N1 and H1N1 challenge with the exception of the AddaVax group against H1N1. The previous work showed the opposite of antigenic competition (the trivalent formulation performed even better against H5N1). This could be explained by the higher antigen dose used in the previous study (3 µg instead of 1 µg in this work) and/or the different adjuvant.

Due to the ambiguous results, it remains difficult to choose an ideal vaccine formulation. If challenged with the same NA as included in the vaccine – monovalent formulations showed higher protection (challenge with H1N1 and H5N1) due to antigenic competition. In the challenge with H1N1 with the exception of the AddaVax group. However, humans are currently confronted with three influenza strains (four including H5N1) and the protection provided by the monovalent formulations was heterologous but not heterosubtypic. By comparing he trivalent formulations, the AddaVax adjuvanted groups performed always better or roughly equal than the SMNP/alum adjuvanted groups.

The approval of new adjuvants by the FDA or EMA is always difficult and requires extensive toxicological data in humans. It is therefore pragmatic to proceed with an adjuvant already licensed in a vaccine. This can be MF59, that is similar to AddaVax or CpG 1018 that showed great promise with similar antigens before[59].

Resources

1. Krammer, F. *et al.* Influenza. *Nat Rev Dis Primers* **4**, 3 (2018).

2. Wu, Y., Wu, Y., Tefsen, B., Shi, Y. & Gao, G. F. Bat-derived influenza-like viruses H17N10 and H18N11. *Trends in Microbiology* **22**, 183–191 (2014).

3. Gamblin, S. J. & Skehel, J. J. Influenza Hemagglutinin and Neuraminidase Membrane Glycoproteins. *Journal of Biological Chemistry* **285**, 28403–28409 (2010).

4. Takemoto, D. K., Skehel, J. J. & Wiley, D. C. A Surface Plasmon Resonance Assay for the Binding of Influenza Virus Hemagglutinin to Its Sialic Acid Receptor. *Virology* **217**, 452–458 (1996).

5. Liu, L. Fields Virology, 6th Edition. *Clinical Infectious Diseases* **59**, 613–613 (2014).

6. Bullough, P. A., Hughson, F. M., Skehel, J. J. & Wiley, D. C. Structure of influenza haemagglutinin at the pH of membrane fusion. *Nature* **371**, 37–43 (1994).

7. Portela, A. & Digard, P. The influenza virus nucleoprotein: a multifunctional RNA-binding protein pivotal to virus replication. *Journal of General Virology* **83**, 723–734 (2002).

8. Martin, K. & Helenius, A. Transport of incoming influenza virus nucleocapsids into the nucleus. *J Virol* **65**, 232–244 (1991).

9. Ma, W., Kahn, R. E. & Richt, J. A. The pig as a mixing vessel for influenza viruses: Human and veterinary implications. *J Mol Genet Med* **3**, 158–166 (2008).

10. Xiong, X., McCauley, J. W. & Steinhauer, D. A. Receptor Binding Properties of the Influenza Virus Hemagglutinin as a Determinant of Host Range. in *Influenza Pathogenesis and Control - Volume I* (eds. Compans, R. W. & Oldstone, M. B. A.) vol. 385 63–91 (Springer International Publishing, 2014).

11. Chen, Y.-Q. *et al.* Influenza Infection in Humans Induces Broadly Cross-Reactive and Protective Neuraminidase-Reactive Antibodies. *Cell* **173**, 417-429.e10 (2018).

12. Krammer, F. *et al.* NAction! How Can Neuraminidase-Based Immunity Contribute to Better Influenza Virus Vaccines? *mBio* **9**, e02332-17.

13. DiazGranados, C. A., Decker, M. D., Chit, A., Mercer, M. & Greenberg, D. P. Fluzone® High-Dose Influenza Vaccine. *Expert Review of Vaccines* **15**, 1495–1505 (2016).

14. Khurana, S. *et al.* MF59 Adjuvant Enhances Diversity and Affinity of Antibody-Mediated Immune Response to Pandemic Influenza Vaccines. *Sci. Transl. Med.* **3**, (2011).

15. Sasaki, S. *et al.* Distinct Cross-reactive B-Cell Responses to Live Attenuated and Inactivated Influenza Vaccines. *The Journal of Infectious Diseases* **210**, 865–874 (2014).

16. Caspard, H., Mallory, R. M., Yu, J. & Ambrose, C. S. Live-Attenuated Influenza Vaccine Effectiveness in Children From 2009 to 2015–2016: A Systematic Review and Meta-Analysis. *Open Forum Infectious Diseases* **4**, ofx111 (2017).

17. Pebody, R., McMenamin, J. & Nohynek, H. Live attenuated influenza vaccine (LAIV): recent effectiveness results from the USA and implications for LAIV programmes elsewhere. *Arch Dis Child* **103**, 101–105 (2018).

18. Lamb, Y. N. Cell-Based Quadrivalent Inactivated InfluenzaVirus Vaccine (Flucelvax® Tetra/FlucelvaxQuadrivalent®): A Review in the Prevention ofInfluenza. *Drugs* **79**, 1337–1348 (2019).

19. Iuliano, A. D. *et al.* Estimates of global seasonal influenza-associated respiratory mortality: a modelling study. *The Lancet* **391**, 1285–1300 (2018).

20. Flannery, B. *et al.* Influenza Vaccine Effectiveness Against Pediatric Deaths: 2010–2014. *Pediatrics* **139**, e20164244 (2017).

21. CDC Seasonal Flu Vaccine Effectiveness Studies | CDC. https://www.cdc.gov/flu/vaccines-work/effectiveness-studies.htm (2022).

22. Wrammert, J. *et al.* Rapid cloning of high-affinity human monoclonal antibodies against influenza virus. *Nature* **453**, 667–671 (2008).

23. Zarnitsyna, V. I. *et al.* Masking of antigenic epitopes by antibodies shapes the humoral immune response to influenza. *Phil. Trans. R. Soc. B* **370**, 20140248 (2015).

24. Saito, N. *et al.* Negative impact of prior influenza vaccination on current influenza vaccination among people infected and not infected in prior season: A test-negative case-control study in Japan. *Vaccine* **35**, 687–693 (2017).

25. Matrosovich, M. N., Matrosovich, T. Y., Gray, T., Roberts, N. A. & Klenk, H.-D. Neuraminidase Is Important for the Initiation of Influenza Virus Infection in Human Airway Epithelium. *J Virol* **78**, 12665–12667 (2004).

26. McMahon, M. *et al.* Mucosal Immunity against Neuraminidase Prevents Influenza B Virus Transmission in Guinea Pigs. *mBio* **10**, e00560-19 (2019).

27. Stadlbauer, D. *et al.* Broadly protective human antibodies that target the active site of influenza virus neuraminidase. *Science* **366**, 499–504 (2019).

28. Couch, R. B. *et al.* Antibody correlates and predictors of immunity to naturally occurring influenza in humans and the importance of antibody to the neuraminidase. *J Infect Dis* **207**, 974–981 (2013).

29. Memoli, M. J. *et al.* Evaluation of Antihemagglutinin and Antineuraminidase Antibodies as Correlates of Protection in an Influenza A/H1N1 Virus Healthy Human Challenge Model. *mBio* **7**, (2016).

30. He, W. *et al.* Epitope specificity plays a critical role in regulating antibody-dependent cell-mediated cytotoxicity against influenza A virus. *Proc. Natl. Acad. Sci. U.S.A.* **113**, 11931–11936 (2016).

31. Cox, F. *et al.* HA Antibody-Mediated FcγRIIIa Activity Is Both Dependent on FcR Engagement and Interactions between HA and Sialic Acids. *Front. Immunol.* **7**, (2016).

32. Zheng, A. *et al.* Enhancing Neuraminidase Immunogenicity of Influenza A Viruses by Rewiring RNA Packaging Signals. *J Virol* **94**, e00742-20 (2020).

33. Broecker, F. *et al.* Extending the Stalk Enhances Immunogenicity of the Influenza Virus Neuraminidase. *J Virol* **93**, (2019).

34. Smith, G. E. *et al.* Neuraminidase-based recombinant virus-like particles protect against lethal avian influenza A(H5N1) virus infection in ferrets. *Virology* **509**, 90–97 (2017).

35. Easterbrook, J. D. *et al.* Protection against a lethal H5N1 influenza challenge by intranasal immunization with virus-like particles containing 2009 pandemic H1N1 neuraminidase in mice. *Virology* **432**, 39–44 (2012).

36. Job, E. R. *et al.* Broadened immunity against influenza by vaccination with computationally designed influenza virus N1 neuraminidase constructs. *npj Vaccines* **3**, 55 (2018).

37. Oleszycka, E. & Lavelle, E. C. Immunomodulatory properties of the vaccine adjuvant alum. *Current Opinion in Immunology* **28**, 1–5 (2014).

38. HogenEsch, H., O'Hagan, D. T. & Fox, C. B. Optimizing the utilization of aluminum adjuvants in vaccines: you might just get what you want. *npj Vaccines* **3**, 51 (2018).

39. Moyer, T. J. *et al.* Engineered immunogen binding to alum adjuvant enhances humoral immunity. *Nat Med* **26**, 430–440 (2020).

40. Rodrigues, K. A. *et al.* Phosphate-mediated coanchoring of RBD immunogens and molecular adjuvants to alum potentiates humoral immunity against SARS-CoV-2. *Sci. Adv.* **7**, eabj6538 (2021).

41. Osbourn, A. Saponins and plant defence — a soap story. *Trends in Plant Science* **1**, 4–9 (1996).

42. *Immunopotentiators in modern vaccines*. (Elsevier/AP, Academic Press is an imprint of Elsevier, 2017).

43. Silva, M. *et al.* A particulate saponin/TLR agonist vaccine adjuvant alters lymph flow and modulates adaptive immunity. *Sci. Immunol.* **6**, eabf1152 (2021).

44. Fries, L. F., Smith, G. E. & Glenn, G. M. A Recombinant Viruslike Particle Influenza A (H7N9) Vaccine. *N Engl J Med* **369**, 2564–2566 (2013).

45. Goscianska, J., Freund, R. & Wuttke, S. Nanoscience versus Viruses: The SARS-CoV-2 Case. *Adv Funct Materials* **32**, 2107826 (2022).

46. Leighton, J., Estes, L. W., Mansukhani, S. & Brada, Z. A cell line derived from normal dog kidney (MDCK) exhibiting qualities of papillary adenocarcinoma and of renal tubular epithelium. *Cancer* **26**, 1022–1028 (1970).

47. Strohmeier, S. *et al.* A Novel Recombinant Influenza Virus Neuraminidase Vaccine Candidate Stabilized by a Measles Virus Phosphoprotein Tetramerization Domain Provides Robust Protection from Virus Challenge in the Mouse Model. *mBio* **12**, e02241-21 (2021).

48. Margine, I., Palese, P. & Krammer, F. Expression of functional recombinant hemagglutinin and neuraminidase proteins from the novel H7N9 influenza virus using the baculovirus expression system. *J Vis Exp* e51112 (2013) doi:10.3791/51112.

49. Cirelli, K. M. *et al.* Slow Delivery Immunization Enhances HIV Neutralizing Antibody and Germinal Center Responses via Modulation of Immunodominance. *Cell* **177**, 1153-1171.e28 (2019).

50. Influenza Virus Research Center-National Institute of Infectious Diseases. Influenza Vaccine Strains for Japan. (Japanese). https://www.niid.go.jp/niid/ja/vaccine-j/249-vaccine/584-atpcs002.html.

51. Maines, T. R. *et al.* Avian Influenza (H5N1) Viruses Isolated from Humans in Asia in 2004 Exhibit Increased Virulence in Mammals. *Journal of Virology* **79**, 11788–11800 (2005).

52. Liu, Y. *et al.* Mosaic Hemagglutinin-Based Whole Inactivated Virus Vaccines Induce Broad Protection Against Influenza B Virus Challenge in Mice. *Front. Immunol.* **12**, 746447 (2021).

53. Killian, M. L. Hemagglutination Assay for Influenza Virus. in *Animal Influenza Virus* (ed. Spackman, E.) vol. 1161 3–9 (Springer New York, 2014).

54. Galani, I.-E., Triantafyllia, V., Eleminiadou, E.-E. & Andreakos, E. Protocol for influenza A virus infection of mice and viral load determination. *STAR Protocols* **3**, 101151 (2022).

55. Reed, L. J. & Muench, H. A SIMPLE METHOD OF ESTIMATING FIFTY PER CENT ENDPOINTS12. *American Journal of Epidemiology* **27**, 493–497 (1938).

56. Koutsakos, M., Wheatley, A. K., Laurie, K., Kent, S. J. & Rockman, S. Influenza lineage extinction during the COVID-19 pandemic? *Nat Rev Microbiol* **19**, 741–742 (2021).

57. Peiris, J. S. M., de Jong, M. D. & Guan, Y. Avian Influenza Virus (H5N1): a Threat to Human Health. *Clin Microbiol Rev* **20**, 243–267 (2007).

58. Morens, D. M., Taubenberger, J. K., Folkers, G. K. & Fauci, A. S. Pandemic Influenza's 500th Anniversary. *CLIN INFECT DIS* **51**, 1442–1444 (2010).

59. Strohmeier, S. *et al.* A CpG 1018 adjuvanted neuraminidase vaccine provides robust protection from influenza virus challenge in mice. *npj Vaccines* **7**, 81 (2022).

60. Wang, C. *et al.* Germinal Center B Cell and T Follicular Helper Cell Responses to Viral Vector and Protein-in-Adjuvant Vaccines. *J.I.* **197**, 1242–1251 (2016).

61. Reif, K. *et al.* Balanced responsiveness to chemoattractants from adjacent zones determines B-cell position. *Nature* **416**, 94–99 (2002).

62. MacLennan, I. C. M. *et al.* Extrafollicular antibody responses: MacLennan et al · Extrafollicular antibody responses. *Immunological Reviews* **194**, 8–18 (2003).

63. *Plotkin's Vaccines*. (Elsevier, 2018). doi:10.1016/C2013-0-18914-3.

64. Deenick, E. K., Hasbold, J. & Hodgkin, P. D. Decision criteria for resolving isotype switching conflicts by B cells. *Eur. J. Immunol.* **35**, 2949–2955 (2005).

65. Calabro, S. *et al.* The adjuvant effect of MF59 is due to the oil-in-water emulsion formulation, none of the individual components induce a comparable adjuvant effect. *Vaccine* **31**, 3363–3369 (2013).